Plant Communications, Volume *4*

Supplemental information

An enhanced network of energy metabolism, lysine acetylation, and growth-promoting protein accumulation is associated with heterosis in elite hybrid rice

Xuan Ma, Qingxiao Jia, Sheng Li, Zhengting Chen, Xin Ming, Yu Zhao, and Dao-Xiu Zhou

Supplemental information

An enhanced network of energy metabolism, lysine acetylation and growth-promoting protein accumulation is associated with heterosis in elite hybrid rice

Xuan Ma[1], Qingxiao Jia[1], Sheng Li[1], Zhengting Chen[1], Xin Ming[1], Yu Zhao[1], Dao-Xiu Zhou[1,2]*

[1] National Key Laboratory of Crop Genetic Improvement, Hubei Hongshan Laboratory, Huazhong Agricultural University, 430070 Wuhan, China

[2] Institute of Plant Science Paris-Saclay (IPS2), CNRS, INRAE, University Paris-Saclay, 91405 Orsay, France

*Correspondence: Dao-Xiu Zhou (dao-xiu.zhou@universite-paris-saclay.fr)

Supplemental Figures: 1~11

Supplemental Tables: 1~4

Supplemental Figures

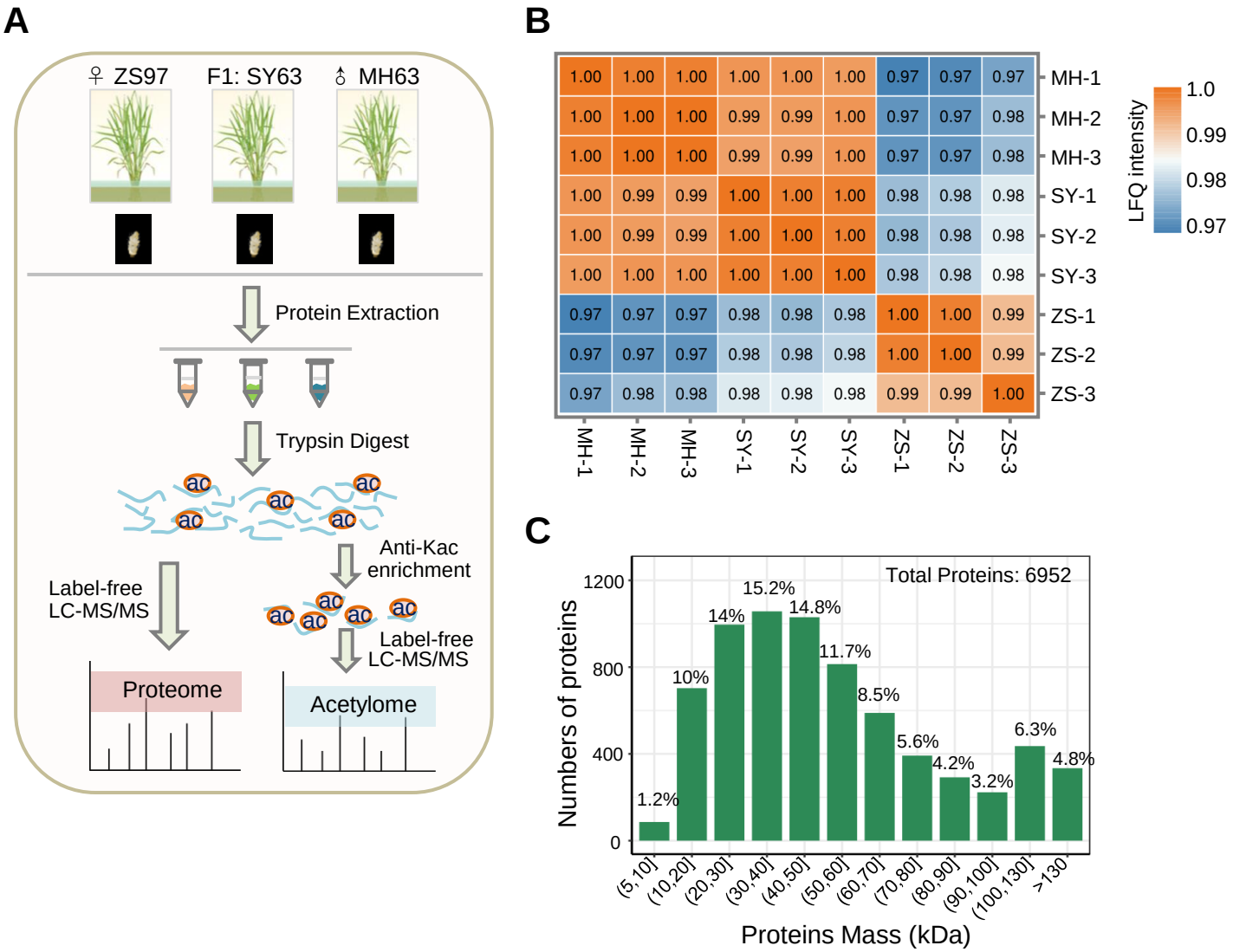

Supplemental Figure 1. Quality control of proteomes of MH63, ZS97 and the hybrid SY63 panicle meristems. (A) Experimental flowchart of quantitative proteome and lysine-acetylome of panicle samples by LC-MS/MS. **(B)** Heatmap of Pearson correlation coefficients of the 3 proteomic replicates of MH63 (MH), ZS97 (ZS), and SY63 (SY). **(C)** Distribution by molecular weight of the identified proteins.

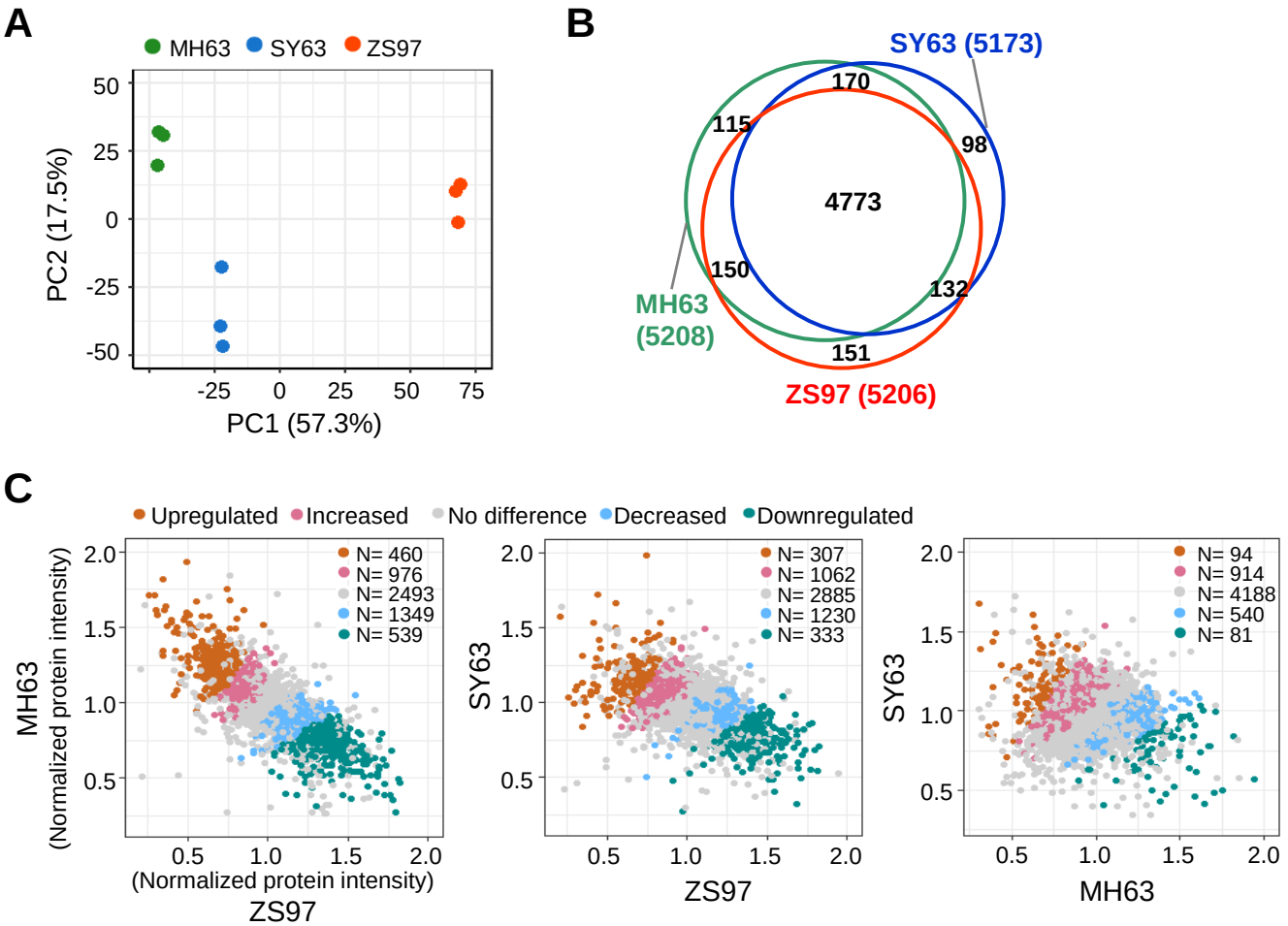

Supplemental Figure 2. Comparison of SY63, MH63, and ZS97 proteomes. (A) PCA analysis of the proteomes of three biological replicates of each genotype are shown. **(B)** Venn diagrams showing overlapped proteins between MH63, SY63 and ZS97. **(C)** Scatter-plot showing the differentially accumulated proteins in MH63 *vs.* ZS97, SY63 *vs.* ZS97 and SY63 *vs.* MH63. Fold change (FC) ≥ 1.5 and $P < 0.05$ (Two tailed t-test) was defined as up-regulated, $1 < FC < 1.5$ and $P < 0.05$ was defined as increased, $0.667 < FC < 1$ and $P < 0.05$ was defined as decreased, $0 < FC < 0.667$ and $P < 0.05$ was defined as downregulated, $FC = 1$ or $P > 0.05$ was defined as no difference.

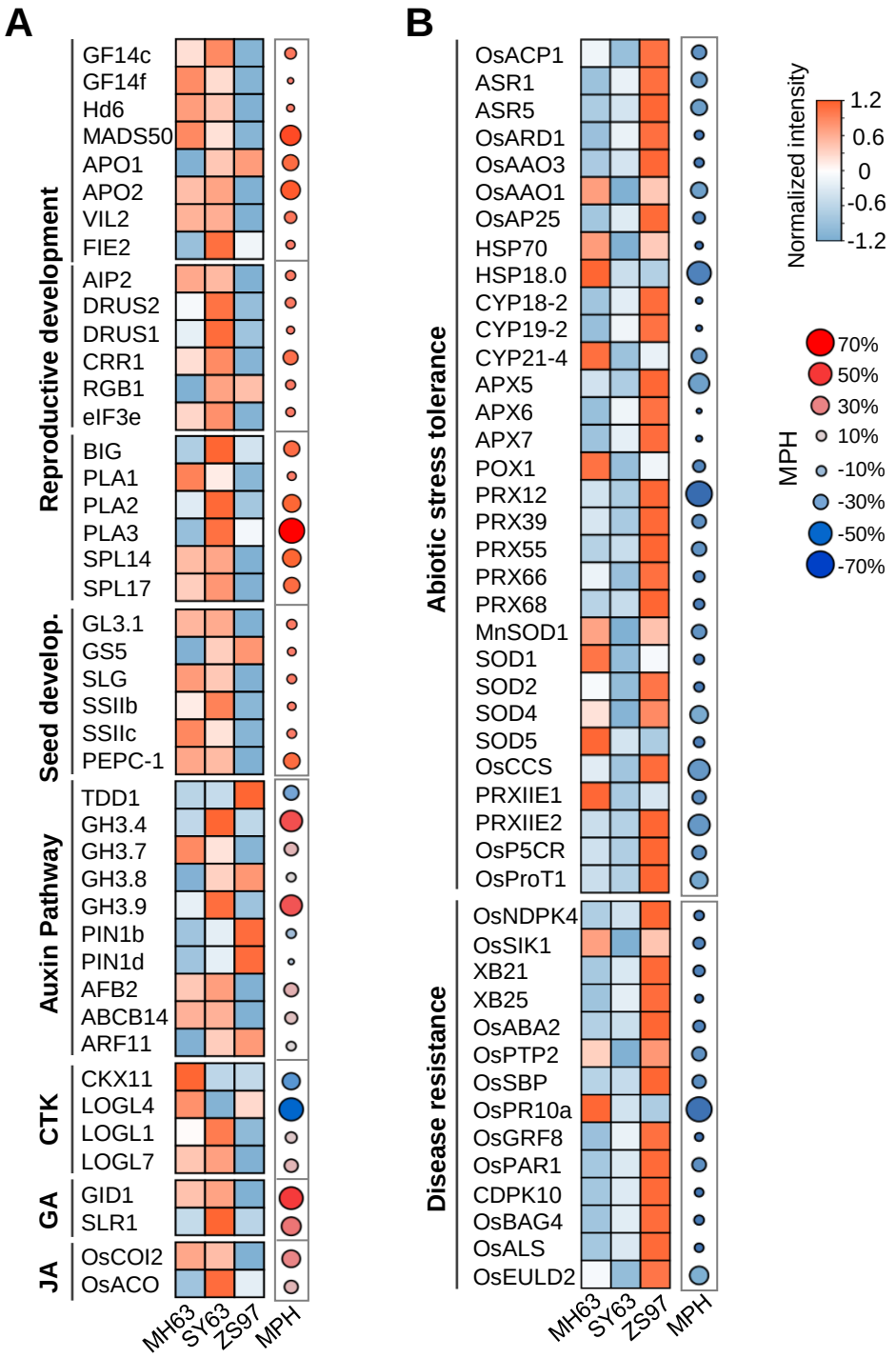

Supplemental Figure 3. (A) Heatmap showing heterotic accumulation of proteins involved in reproductive development, starch synthesis, and hormone signaling pathways in SY63 relative to MH63 and ZS97. **(B)** Heatmap showing of abiotic and biotic stress proteins that were reduced in SY63 panicle.

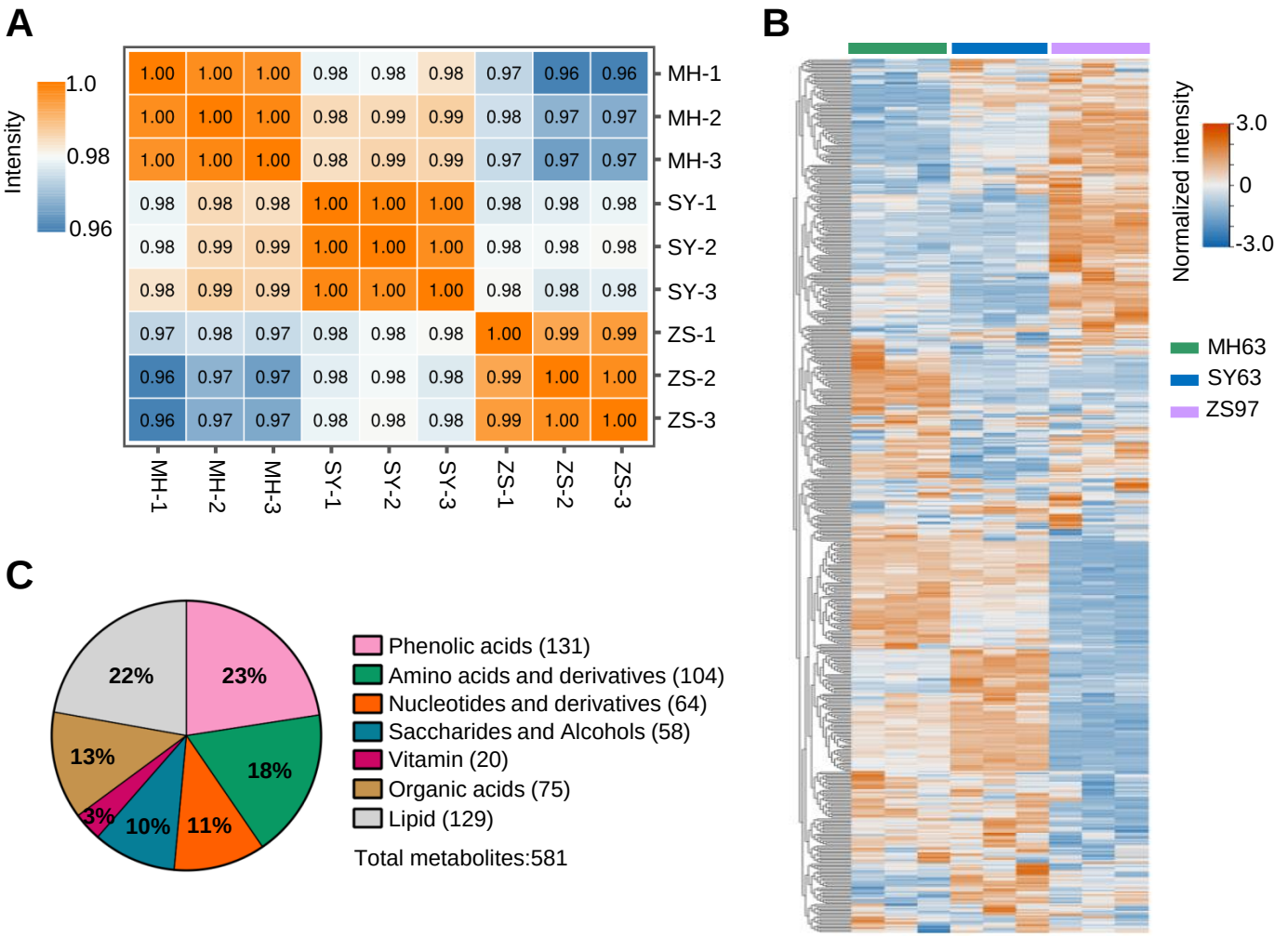

Supplemental Figure 4. Primary metabolomic analysis of MH63, ZS97 and the hybrid SY63 young panicles. (A) Metabolomic replicates and Pearson correlation coefficients of MH63 (MH), SY63 (SY) and ZS97 (ZS). **(B)** Heatmap of the overall primary metabolites detected in MH63, SY63, and ZS97 young panicles. **(C)** Percentage of different types of the primary metabolites identified in the panicles.

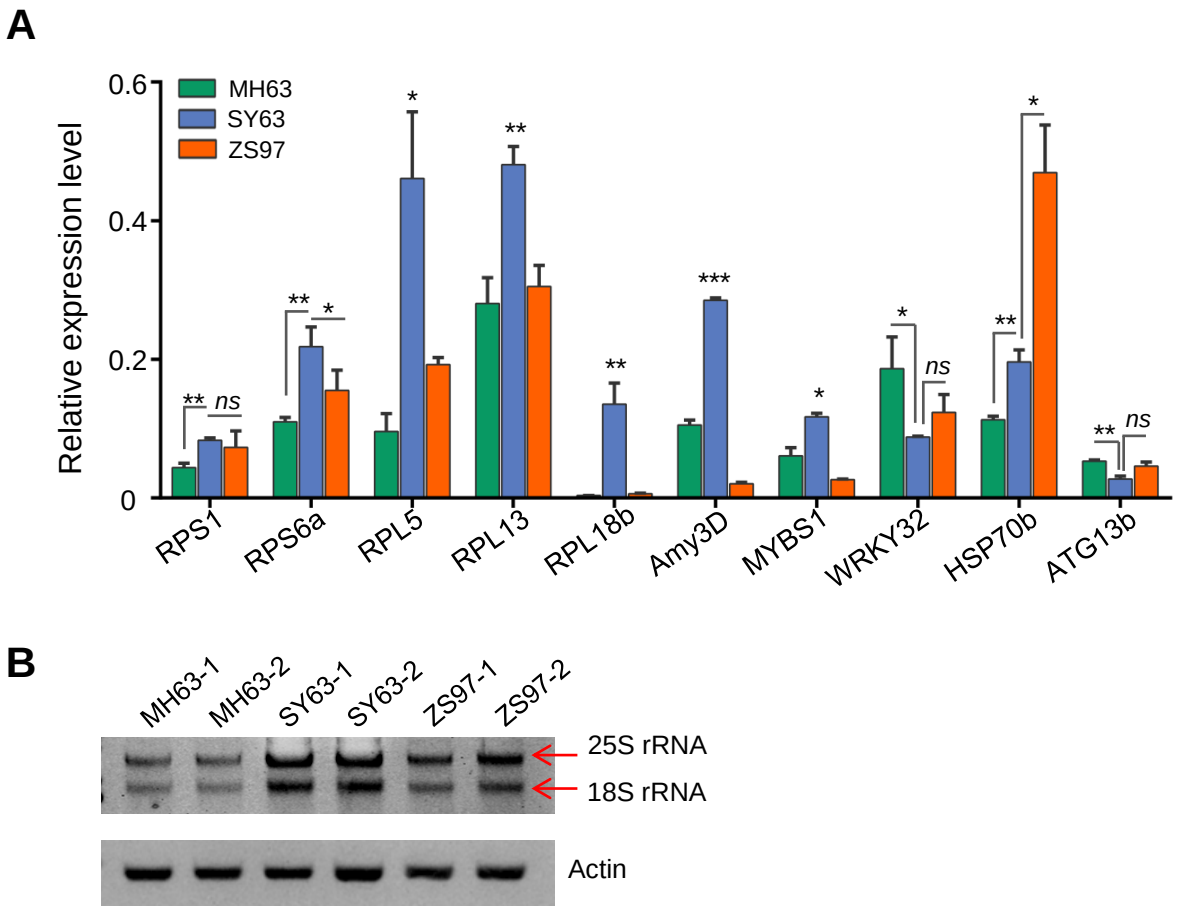

Supplemental Figure 5. Relative expression levels of the genes related to TOR signaling and the rRNA abundance in MH63, ZS97 and the hybrid SY63 young panicles. (A) Real-time quantitative PCR (RT-qPCR) analysis of the expression of ribosomal genes (RPS1, RPS6a, RPL5, RPL13 and RPL18b) and energy metabolism related genes (relative to *Actin*). Bars indicate means ± SD from three replicates. *, $P < 0.05$, **, $P < 0.01$, ***, $P < 0.001$, *ns*, $P > 0.05$ (Two tailed t-test). **(B)** Agarose gel electrophoresis detection of rRNA abundance in MH63, SY63, and ZS97 young panicles (total RNA extracted with 100 mg FW of panicle meristem). Two biological replicates are shown.

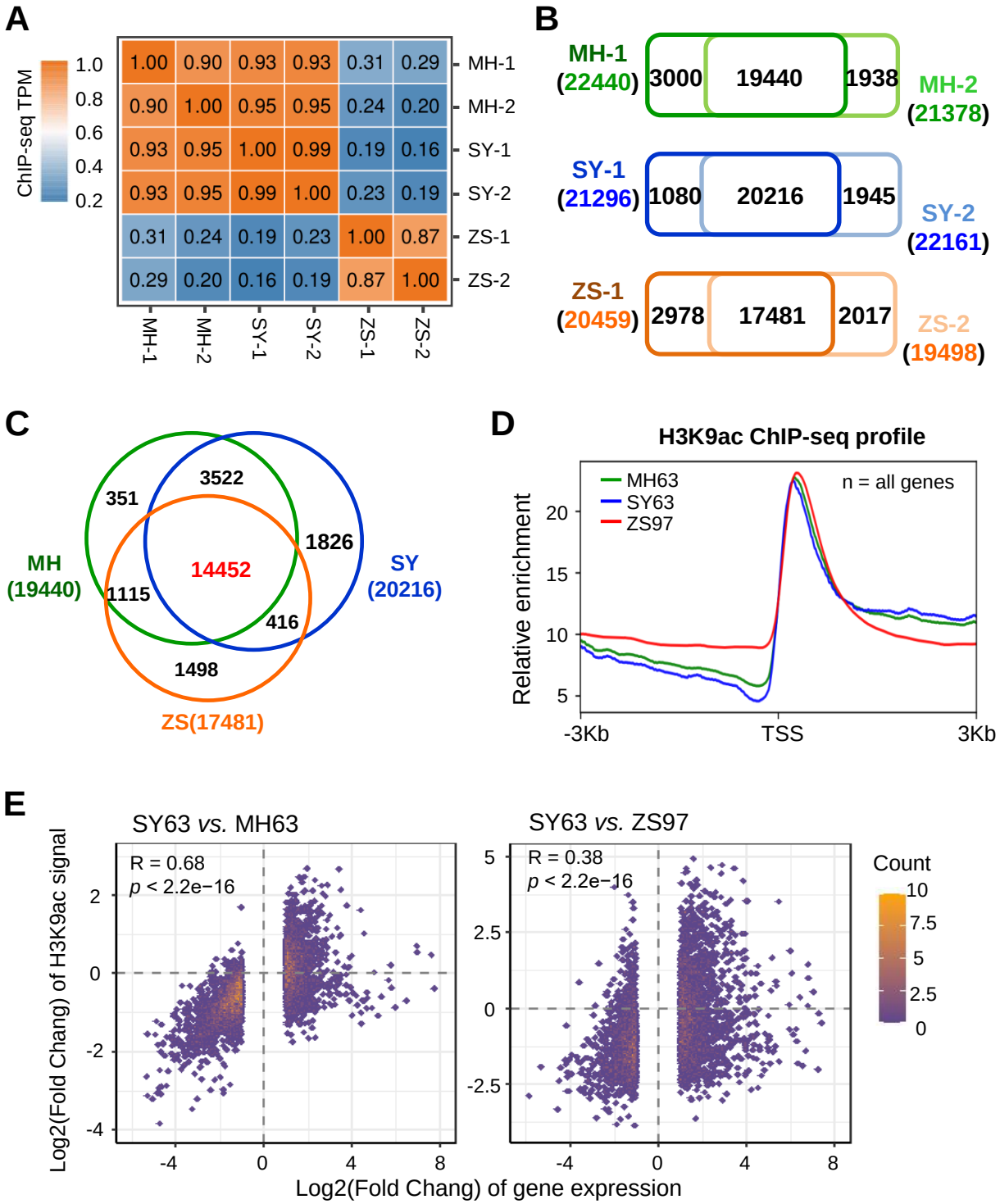

Supplemental Figure 6. H3K9ac ChIP-seq analysis of MH63, SY63 and ZS97. (A) Correlation matrix of MH63 (MH), SY63 (SY) and ZS97 (ZS) ChIP-seq replicates. Pearson correlation coefficient was calculated by TPM. **(B)** Venn diagrams showing overlapped genes with H3K9ac modification in the two replicates of each genotype. **(C)** Venn diagram showing overlapping of the H3K9ac modified genes between MH63, SY63 and ZS97. **(D)** Metaplots of genic H3K9ac levels in MH63, SY63 and ZS97. **(E)** Scatter-plot showing the changes of H3K9ac (Fold change of TPM) between SY63 and the parents was positively correlated to gene expression (Fold change of FPKM).

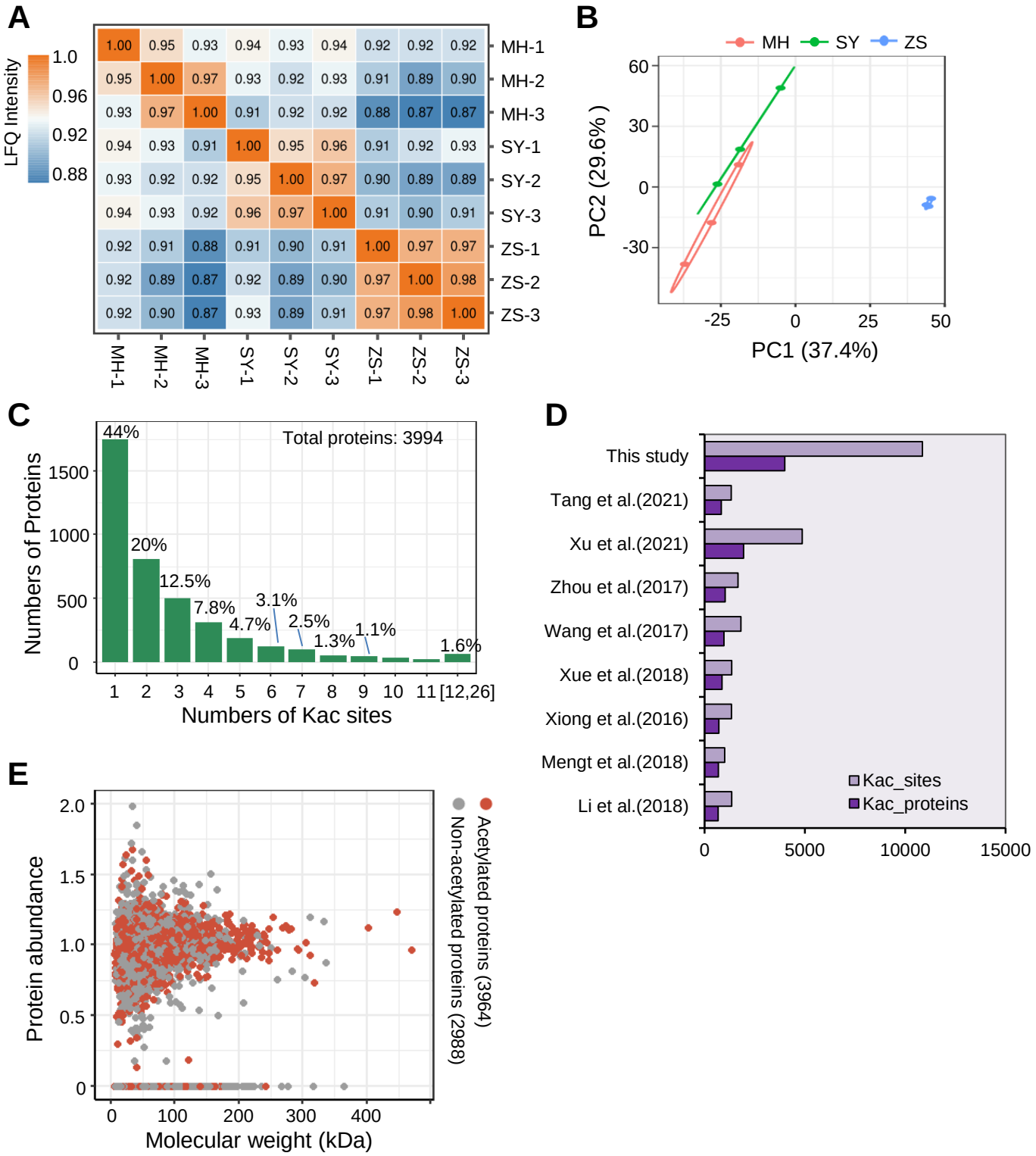

Supplemental Figure 7. Quality control and analysis of protein lysine acetylome of MH63, ZS97 and the hybrid SY63 panicle meristems. (A) Heatmap of Pearson correlations of the 3 replicates for each genotype. **(B)** PCA analysis of the acetylomes from the three genotypes. **(C)** Distribution of the lysine acetylation (Kac) sites of proteins identified in acetylome. **(D)** The numbers of Kac sites and acetylated proteins identified in the study and previous ones in rice. **(E)** Scatter-plot showing distribution of the acetylated proteins and all proteins by molecular mass.

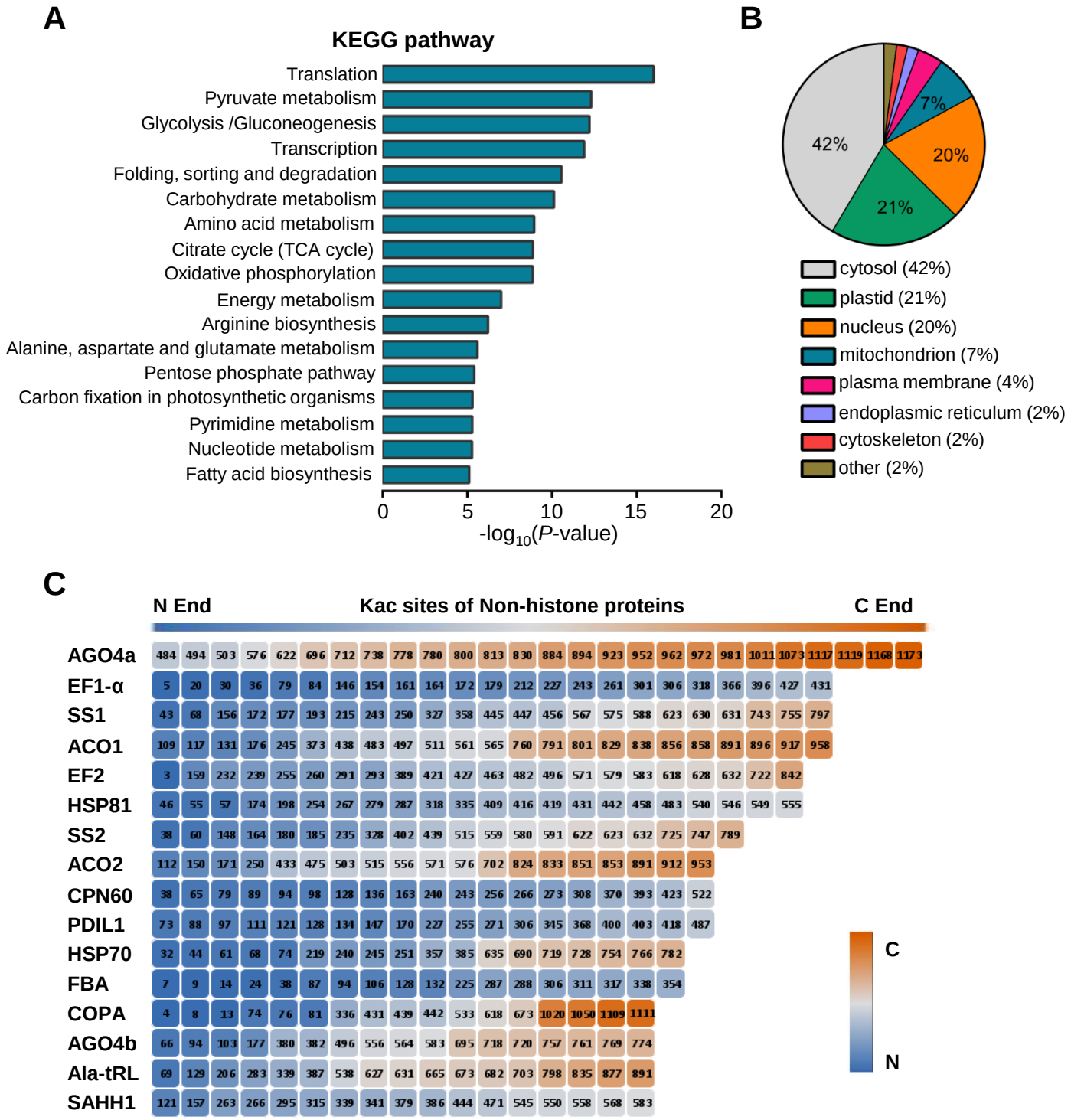

Supplemental Figure 8. Characterization of acetylated proteins in rice panicles. (A) KEGG pathway enrichment of the acetylated proteins in rice panicle. **(B)** Subcellular localization prediction of the acetylated proteins. **(C)** The hyper-acetylated proteins and the Kac sites (without histone, Kac sites ≥ 17 are shown) identified in the rice panicles.

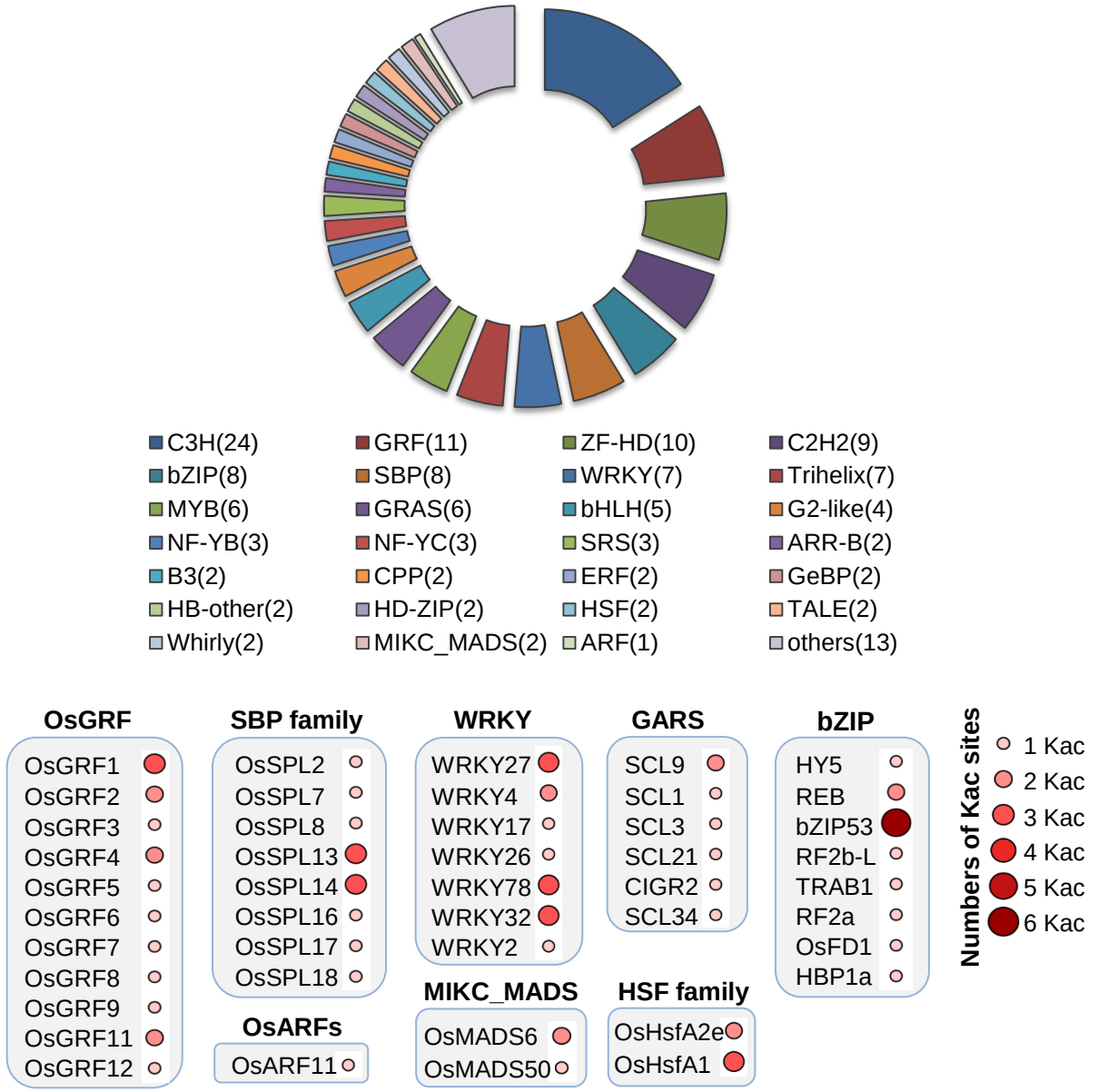

Supplemental Figure 9. Acetylated transcription factors in the rice panicles.

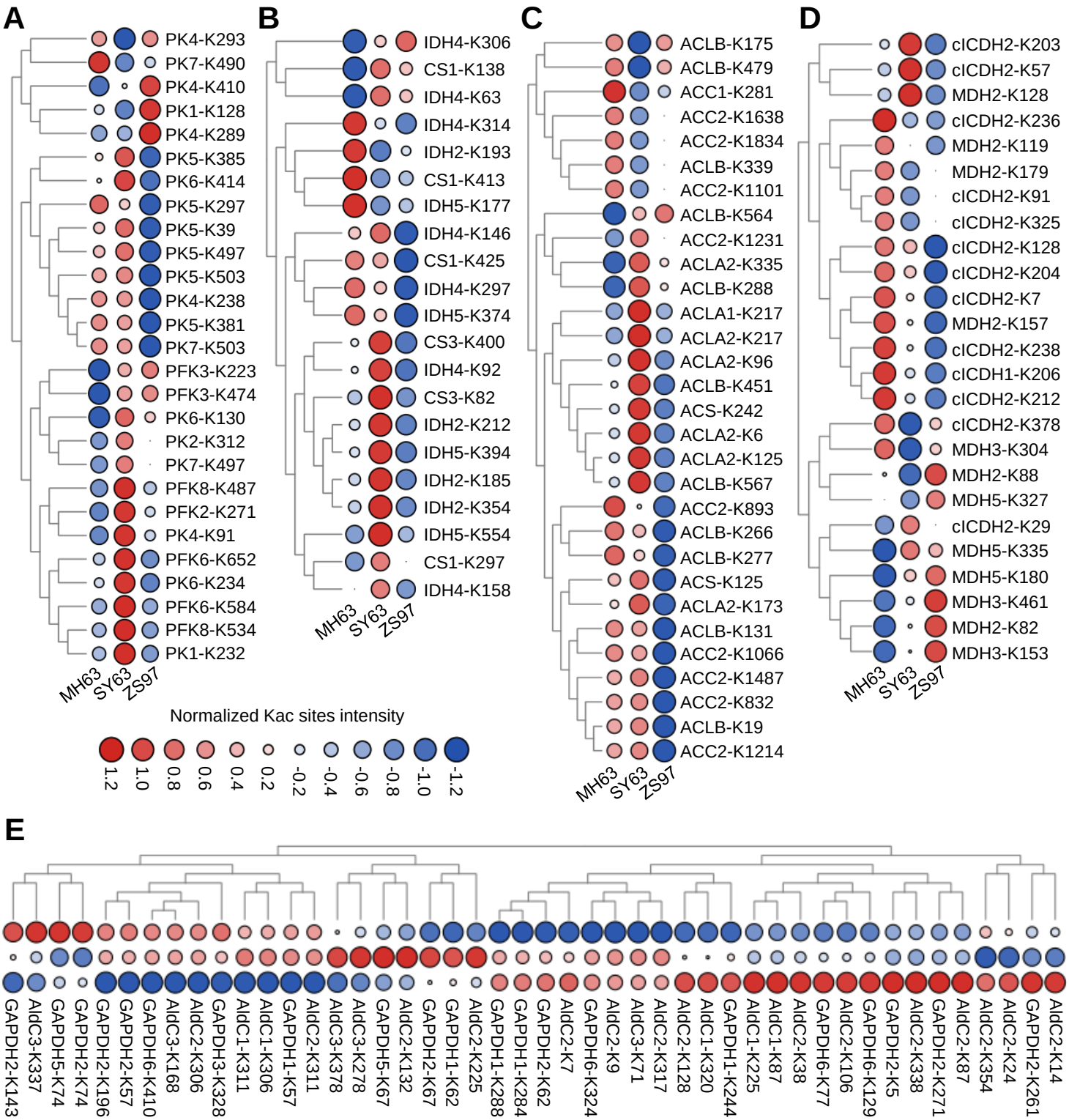

Supplemental Figure 10. Lysine acetylation (Kac) levels of enzymes in glycolysis, TCA and acetyl-CoA synthesis in MH63, SY63 and ZS97 panicles. As shown the heatmaps of Kac levels of **(A)** phosphofructokinase (PFK), pyruvate kinase (PK), **(B)** citrate synthase (CS), isocitrate dehydrogenase (IDH), **(C)** ATP-citrate lyase (ACLA/B), acetyl-coenzyme A synthetase (ACS), acetyl-CoA carboxylase (ACC), **(D)** cytosolic isocitrate dehydrogenase (cICDH), malate dehydrogenase (MDH), **(E)** glyceraldehyde-3-phosphate dehydrogenase (GAPDH) and fructose-bisphosphate aldolase (AldC) in the three genotypes.

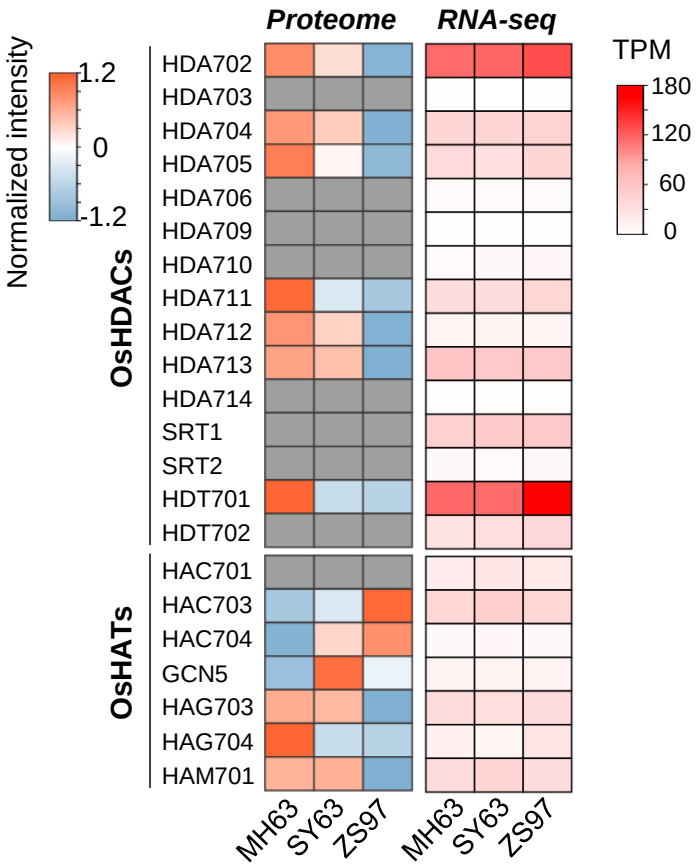

Supplemental Figure 11. Heatmap showing the protein abundance (left) and transcript levels (right) of rice histone acetyltransferases (OsHATs) and deacetylase (OsHDACs) in MH63, ZS97 and SY63 young panicles.

Supplemental References (Related to Supplemental Fig. 7D)

Tang, B., liu C., Li, Z., Zhang, X., Zhou, S., Wang, G.L., Chen, X.L., Liu, W. (2021). Multilayer regulatory landscape during pattern-triggered immunity in rice. Plant Biotechnol J 19: 2629-2645.

Xu, Q., Liu, Q., Chen, Z., Yue, Y., Liu, Y., Zhao, Y., Zhou, D.X. (2021). Histone deacetylases control lysine acetylation of ribosomal proteins in rice. Nucleic Acids Res 49:4613–4628.

Zhou, H., Finkemeier, I., Guan, W., Tossounianet, M.A., Wei, B., Young, D., Huang, J., Messens, J., Yang, X., Zhu, J. et al (2018). Oxidative stress-triggered interactions between the succinyl-and acetyl-proteomes of rice leaves. Plant Cell Environ 41:1139–1153.

Wang, Y., Hou, Y., Qiu, J., Li, Z., Zhao, J., Tong, X., Zhang, J. (2017). A Quantitative Acetylomic Analysis of Early Seed Development in Rice (*Oryza sativa* L.). Int J Mol Sci 18, 1376.

Xue, C., Liu, S., Chen, C., Zhu, J., Yang, X., Zhou, Y., Guo, R., Liu, X., Gong, Z. (2018). Global Proteome Analysis Links Lysine Acetylation to Diverse Functions in *Oryza Sativa*. Proteomics 18, 1700036.

Xiong, Y., Peng, X., Cheng, Z., Liu, W., Wang, G.L. (2016). A comprehensive catalog of the lysine-acetylation targets in rice (*Oryza sativa*) based on proteomic analyses. J Proteomics 138: 20-29.

Meng, X., Lv, Y., Mujahid, H., Edelmann, M.J., Zhao, H., Peng, X., Peng, Z. (2018). Proteome-wide lysine acetylation identification in developing rice (*Oryza sativa*) seeds and protein co-modification by acetylation, succinylation, ubiquitination, and phosphorylation. BBA – Proteins Proteom 1866: 451–463.

Li, X., Ye, J., Ma, H., Lu, P. (2018). Proteomic analysis of lysine acetylation provides strong evidence for involvement of acetylated proteins in plant meiosis and tapetum function. Plant J 93: 142–154.

Supplemental Tables

Supplemental Table 1. Summary of the MS/MS spectrum raw data.

	Total spectrum	Matched spectrum	Peptides	Unique/modified peptides	Identified proteins	Quantifiable proteins	Identified Kac sites	Quantifiable Kac sites	Normalized proteins	Normalized Kac sites
Proteome	1,780,842	293,520	43,713	40,155	6,952	5,725	NA	NA	NA	NA
Acetylome	464,470	91,451	15,132	10,691	3,994	3,222	10,852	7,948	2,290	6,069

Supplemental Table 2. Summary of H3K9ac ChIP-seq raw data.

Sample	Replicates	Clean reads (millions)	Uniquely aligned reads (millions)	Total aligned reads (millions)	Total peaks	Modified genes	R-squared TPM (all genes)
MH63	1	63.5	33.7 (53.1%)	43.7 (68.8%)	34,339	22,440	0.904
MH63	2	24.9	12.8 (51.3%)	17.2 (69%)	33,578	21,378	
SY63	1	29.4	15.1 (51.4%)	20.2 (68.9%)	34,481	21,296	0.993
SY63	2	27.4	13.7 (49.9%)	17.4 (63.6%)	34,804	22,161	
ZS97	1	26	14.9 (57.3%)	19.3 (74.3%)	24,669	20,459	0.87
ZS97	2	17.6	10.3 (58.5%)	13.6 (77.5%)	23,315	19,498	

Supplemental Table 3. Lysine acetylation sites and values of TORC1 proteins.

Gene locus	Protein	Kac sites	MH63	SY63	ZS97
OsMH_05G0123700	TOR	K1650	0.816	0.993	NA
		K278	NA	0.918	NA
		K1608	NA	1.486	0.776
OsMH_12G0008800	RAPTOR	K181	1.07	NA	1.213
OsMH_03G0472800	LST8	K50	0.963	0.956	NA
		K278	0.892	1.265	0.659
OsMH_02G0526800	FKBP12	K21	0.641	0.89	1.451
		K37	NA	1.081	0.628
		K31	0.764	1.0897	1.113

Supplemental Table 4. Primers used RT-qPCR.

Primer name	Sequence(5'-3')
RPS1-F	TTGAGGTGGAGCTGATAAACTG
RPS1-R	TGCTTGAAGAGTGAAGGATCG
RPS6a-F	CGATCACTGAAGACTGCTCTC
RPS6a-R	ACCAGCGTTCTCCATTTCAC
RPL5-F	GATTGTAGTGAATTGCGGGTTG
RPL5-R	AGTTGAACATTACCCTGCCG
RPL13-F	CGGTCACAGAAGCTCTACAG
RPL13-R	ATGTTCTGCTCCCTTGTACAC
RPL18b-F	CAGTCTGCTCTTTCCTGTCTTC
RPL18b-R	ATGCTCTCGTTGACCTTGG
Amy3D-F	AGCAACTCACTATCGAACACG
Amy3D-R	CGACTTGGCCTTTCAACATG
MYBS1-F	CGAAGACGAGCACAGGTTG
MYBS1-R	GTGATGTCATGGATGCTCTTG
WRKY32-F	AGGTAGTTGAAGTGGTTGTGG
WRKY32-R	TTACCATGTGCTTCTCTTCCG
ATG13b-F	AGCTAGATTTTCGCCACCTC
ATG13b-R	CGAGATTGAAGATACCCGCTG
HSP70b-F	AAGCGGTTGATTGGTAGGAG
HSP70b-R	CTCCCTCATCTTGATCAGCAC
Actin-F	TGTATGCCAGTGGTCGTACCA
Actin-R	CCAGCAAGGTCGAGACGAA